Characterisation of DSB-OCS technique for 40GHz radio over fibre system

Syamsuri Yaakob, Norhakimah Md Samsuri, Nazif Farid, Romli Mohamad, Amiza Rasmi, Muhammad Zamzuri Abdul Kadir
Advanced Physical Technology (APT)
Telekom Research & Development (TM R&D)
Lingkaran Teknokrat Timur, 63000 Cyberjaya, Selangor, Malaysia.
syamsuri@tmrnd.com.my

Sevia Mahdaliza Idrus[1] and Shu-Hao Fan[2]
[1]Faculty of Electrical Engineering Universiti Teknologi Malaysia, Johor 81310, Malaysia
[2]School of Electrical and Computer Engineering, Georgia Institute of Technology, Atlanta, Georgia 30332, USA.
sevia@fke.utm.my

Abstract—**The dual sideband optical carrier suppression (DSB-OCS) technique is characterised for its performance in order to be used as a carrier for 1.25Gbps OOK signal in the 40GHz radio over fibre (ROF) system. A dual electrode Mach-Zehnder modulator (DE-MZM) and the minimum transmission bias (MiTB) technique are employed to build the system. The results show that, a 40GHz carrier is successfully generated with the amplitude up to -29dBm and SNR of 35dB. Finally, an error free 40GHz ROF system is constructed with almost no penalty between the back to back and 20km fibre for a BER of 10^{-9}.**

Keywords-Millimetre wave; Radio over Fibre; Dual Sideband; Optical Carrier Supression; DE-MZM.

I. INTRODUCTION

The millimetre wave (mm-wave) radio over fibre (ROF) system has emerged as the synergy between the optical and wireless technology by offerring gigabit per second (Gbps) wireless access system for future telecommunication use [1-2]. Previously, direct modulation technique is often used to modulate radio frequency (RF) into the optical system to realize the ROF system because of the simplicity in the system design and less costly compared to the external modulation technique using the Mach-Zehnder modulator (MZM). It is done by directly modulating laser diode (LD) current with RF signal. However, there is a limit to the size of bandwidth that can be directly modulated using LD because of the chirp it produces at the frequency of more than 10GHz [3-4]. Therefore, the optical mm-wave generation technique is often adopted to extend the ROF system capability as the frequency is increased to mm-wave region to support Gbps wireless transmission

There are many techniques for the optical mm-wave generation, to name a few, the optical phase-locked loop (OPLL) [5], optical-injection phase-locked loop (OIPLL) [6], dual sideband (DSB) modulation [7], using stimulated Brillouin scattering (SBS) [8-10] and the dual sideband optical carrier suppression (DSB-OCS) [11-14]. The DSB-OCS technique is attractive for mm-wave ROF system because it requires only half of the intended frequency at the central station (CS) to produce the actual mm-wave signal at the remote antenna unit (RAU). It also offers better spectral efficiency, produces tunable mm-wave carrier and utilises fewer and smaller components to generate the optical mm-wave carrier compared to the other techniques mentioned. These factors will give benefit in order to scale done the size of CS and reduce design complexity.

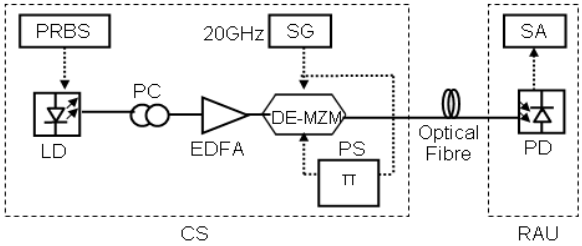

Fig. 1: Setup for the DSB-OCS optical carrier generation technique.

In this paper, we characterize the DSB-OCS technique in order to carry 1.25Gbps OOK signal in the 40GHz ROF system. In the setup, a signal generator is employed to drive the dual electrode Mach-Zehnder modulator (DE-MZM) in order to produce 20GHz sideband. The minimum transmission bias (MiTB) technique is used to suppress the optical carrier so that 40GHz signal can be generated by heterodyne process at the photodetector (PD) which resides at RAU.

II. THEORY

The mm-wave generation using DSB-OCS technique can be achieved by using a DE-MZM. The DE-MZM is an intensity or phase modulator based on $LiNbO_3$ material and a Mach–Zehnder (MZ) interferometer. Assuming the DE-MZM is an ideal device, i.e. no insertion loss, the optical signal at the output of the device can be represented by the equation below:

$$E_{out} = \frac{E_{in}}{\sqrt{2}} \cos\left(\frac{\Delta\phi(t)}{2}\right) . e^{j\Delta\bar{\phi}(t)} . e^{j\Omega t} \quad (1)$$

Where,

$$\Delta\phi(t) = \frac{\pi(V_1(t) - V_2(t))}{V_\pi} \quad (2)$$

$$\Delta\hat{\phi}(t) = \frac{\pi(V_1(t) + V_2(t))}{V_\pi} \quad (3)$$

and E_{in} and E_{out} are the input and output electric field respectively, $V_1(t)$ and $V_2(t)$ are the voltages applied to the electrode 1 and 2 respectively, V_π is the half-wave voltage or the DC voltage required for the optical signal to swing from the maximum to the minimum transmission and Ω is the optical signal frequency. In general, the biasing for MZM is implemented as $V_2(t) = V_{DC} - V_1(t)$. When we consider our operation to be using the bias at the minimum scheme, we use $V_{DC} = V_\pi$, hence, the above equation becomes:

$$E_{out} = -\frac{E_{in}}{\sqrt{2}} \sin\left(\frac{\pi V_1(t)}{V_\pi}\right) e^{j\Omega t} \quad (4)$$

The transfer function of the MZM can also be expressed in term of power of the optical intensity:

$$\frac{P_{out}}{P_{in}} = \frac{1}{4}\left[1 - \left(\cos\left(\frac{2\pi V_1(t)}{V_\pi}\right)\right)\right] e^{j2\Omega t} \quad (5)$$

where P_{in} and P_{out} are the input optical power and output optical power respectively. From this equation, the DSB-OCS output can also be shown as the equation:

$$\frac{P_{out}}{P_{in}} = \frac{1}{2}\sum_{n=1}^{\infty} J_{2n-1}(2\pi m)\sin[(2n-1)w_{RF}t] \quad (6)$$

where $J_n(2\pi m)$ are the Bessel functions of the first kind of nth order, w_{RF} is the RF frequency and m is the RF signal modulation index.

III. EXPERIMENTAL SETUPS

The setup as shown in Fig. 1 is conducted in the laboratory to explore the experimental side of the DSB-OCS technique for the optical mm-wave generation. An LD with a wavelength of 1550.71 nm is used to generate continuous wave (CW) optical lightwave producing an output power of -10dBm and owning relative intensity noise (RIN) of -110 dB/Hz. The optical CW signal passes through a polarization controller in order to maximize the optical signal coupling into the DE-MZM and at the same time ensuring the less possible polarization dependant loss. Next, the signal is amplified by an erbium doped fibre amplifier (EDFA) for overdriving purpose before it is transmitted into a DE-MZM which is driven by a 20GHz RF signal from a signal generator (SG). Initially, the RF signal is divided equally into two sections by a 3 dB power splitter (PS) and a 180° phase difference is introduced between the divided signals using a phase shifter. The output of the DE-MZM is then launched into a 2m optical fiber with loss of α = 0.21 dB/km, and chromatic dispersion of D = 16 ps/(nm.km) . The optical signal is detected by a high-speed PD with a 3dB bandwidth of 60 GHz and a responsivity of 0.85A/W. The PD output is fed into a spectrum analyzer for monitoring and measurement purposes.

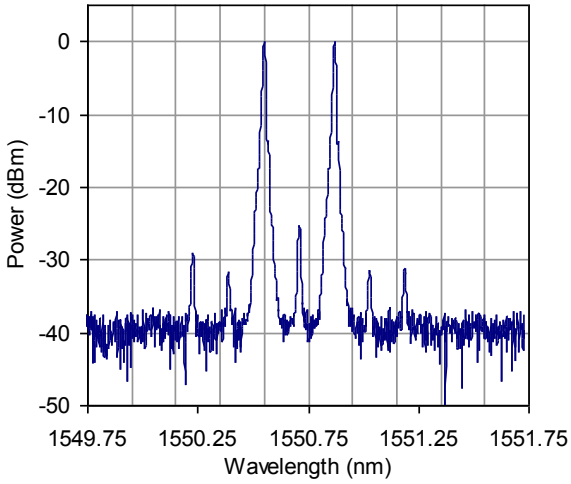

Fig. 2: DE-MZM optical output.

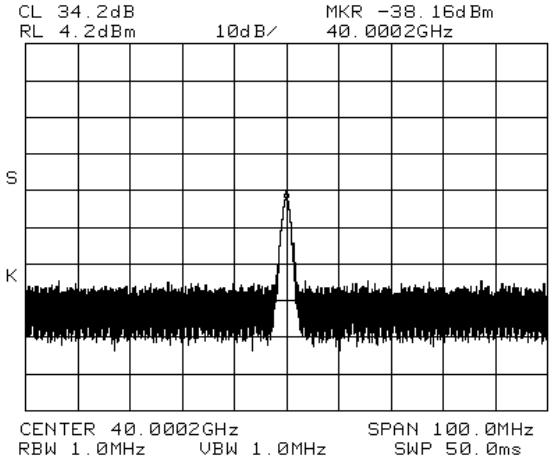

Fig. 3: 40GHz millimetre wave output.

IV. RESULTS AND DISCUSSIONS

The optical output spectrum of DE-MZM is shown in Fig. 2. We can see that the optical carrier suppression is roughly at 25dB. The beating between the optical frequency component (or $\Omega - w$ and $\Omega + w$) results in a mm-wave frequency component at $2w$. In this case, when our w is 20GHz, an output spectrum at 40GHz is obtained as shown in Fig. 3. The amplitude of the mm-wave signal is measured at -38dBm.

The experiment is continued to observe the characteristics for the mm-wave with respect to various optical input power. In this case, the term optical input power refers to the LD output power. Fig. 4 shows that the mm-wave carrier peak power rises almost linearly with the optical input power. For

the case where the driving RF power is at 10dBm, initially the optical power is at 2.5dBm giving mm-wave peak power of -60dBm. The graph rises steadily until the optical input power of 11.5dBm with

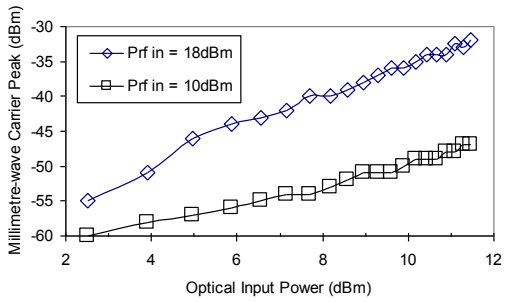

Fig. 4: 40GHz mm-wave output vs optical input power.

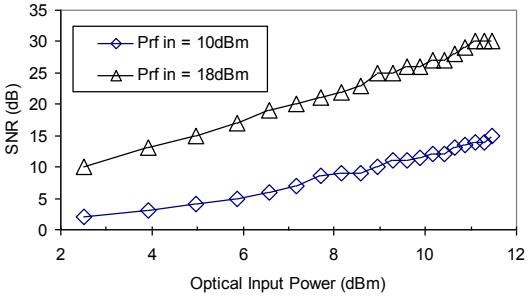

Fig. 5: SNR vs optical input power.

mm peak power of -47dBm. When the driving RF power is changed to 18dBm, the overall graph increases to a higher mm-wave peak power output. Initially -55dBm mm-wave output is observed at the optical power is of 2.5dBm and increasing to -32dBm at the optical input power of 11.5dBm. The generated mm-wave peak power differences for the two driving RF powers are 5dB and 15dB for the optical power of 2.5dBm and 11.5dBm respectively.

The graph in Fig. 5 shows the characteristic of SNR with the optical input power. From the graph, it can be clearly seen that the SNR also behaves the same way as the mm-wave peak power output with respect to the optical input power. When the driving RF power is at 10dBm, optical power of 2.5dBm and 11.5dBm give SNR of 2dBm and 15dBm respectively. Similarly, as the driving RF power is changed to 18dBm, the SNR graph increases with optical input power. The same optical powers of 2.5dBm and 11.5dBm give SNR of 10dBm and 30dBm respectively. The SNR differences for the two driving RF powers are 8dB and 15dB for the optical power of 2.5dBm and 11.5dBm respectively. Next, the experiment is continued by fixing the optical input power at two values which are 10.4dBm and 11.3dBm and varying the RF power input instead. Fig. 6 shows the characteristic of mm-wave carrier peak with the RF power input. There is merely 1-2dB difference with the curve due to merely small gap between the optical power selection. When the optical input power is at 10.4dBm, RF driving power of 5dBm and 20dBm give mm-wave carrier peak of -56dBm and -31dBm respectively. Similarly, as the optical input power is changed to 11.3dBm, the mm-wave carrier peak graph increases with RF power input. The same RF driving power of 5dBm and 20dBm give mm-wave carrier of -55dBm and -29dBm respectively.

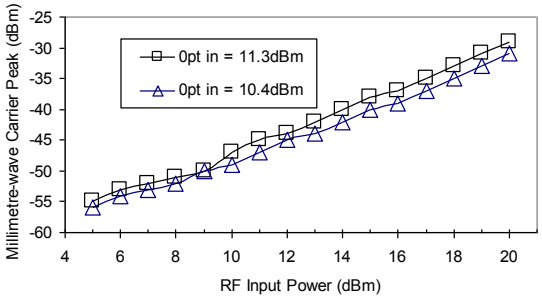

Fig. 6: 40GHz mm-wave output vs RF power input.

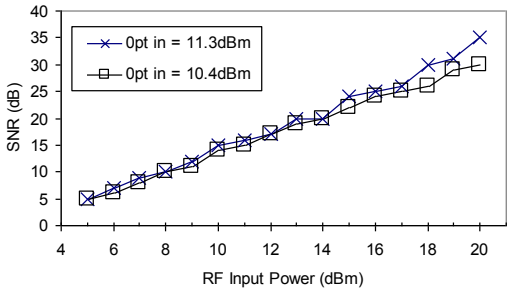

Fig. 7: SNR vs RF power input.

Fig. 7 illustrates the SNR characteristics with different RF power input to the DE-MZM. The SNR for both optical input power (10.4dBm and 11.3dBm) is the same 5dB at RF power input of 5dBm. The curves rises steadily until exhibiting SNR of 30dB and 35dB for the optical input power of 10.4dBm and 11.3dBm, respectively, at RF input power of 20dBm.

TABLE I. DESIGN PARAMETRES

Parameters	**Symbol**	**Value**
Wavelength	λ	1550 nm
LD power	P_{LD}	5 dBm
EDFA current	I_{edfa}	255 mA
DE-MZM Half wave voltage	V_{π}	5.2 V
Drive voltage 1	V_{DC1}	1.18 V
Drive voltage 2	V_{DC2}	0 V
Modulation Voltage 2	V_{RF1}	1Vpp
Modulation Voltage 2	V_{RF2}	1Vpp
Fibre length	L	2 m
PD responsivity	$\mathfrak{R}$	0.85 A/W
Fibre chromatic dispersion	D	16 ps/(nm.km)
Fibre Loss	α	0.21 dB/km

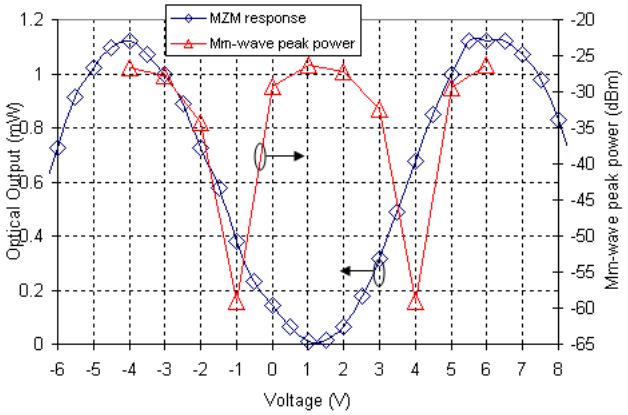

Fig. 8: DE-MZM optical output and mm-wave peak power vs bias voltage.

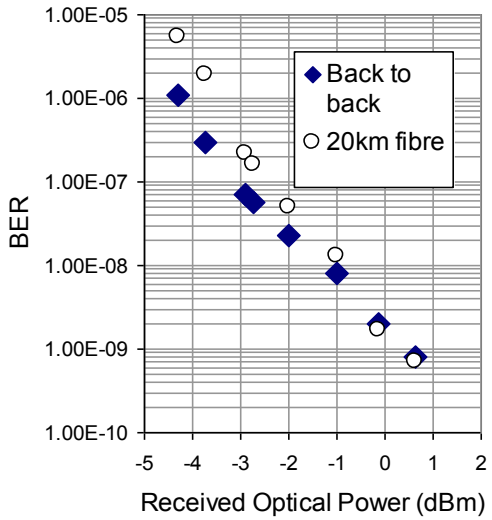

Fig. 9: BER vs received optical power for the mm-wave ROF downlink.

Next, the experiment is repeated with the parameters as given in Table 1. The DE-MZM optical output is plotted together with its associated mm-wave peak power generated to see their responses at different bias voltages as shown in Fig. 8. As predicted, the DE-MZM optical output exhibits the characteristic as DC transfer function of the device. The maximum output of 1.12mW occurs at V_1 = -4V and 6V, whereas the minimum output is observed between 1V to 1.5V. Hence, the half wave voltage for the DE-MZM is in the middle of both voltages which occur at around 1.0V (V_π is around 5V). In ideal case, the minimum output shall be zero because biasing voltage V_1 at this point introduces 180 ^{o} phase shift to the equally split optical signal at the other electrode. The phase shifted signal is then re-combined with the other half which will result in a complete zero output or completely suppressed due to the destructive interference of the two identical waves. However, we can still obtain some output at the minimum bias because of the imperfection of the Y split and combiner of the DE-MZM during its fabrication. Hence, the CW carrier is not completely suppressed. This factor also determines the extinction ratio for the device which is specified at 26dB.

From Fig. 8, it can also be clearly seen that the 40GHz peak power has three maximum points which occur at V_1 = -4V, 1.2V and 6V. This is because at -4V and 6V, the maximum 40GHz mm-wave peak is due to the bias at maximum transmission point. In this case, the heterodyne process to generate the mm-wave signal takes place as a result of beating between the CW component and the dominant 40GHz sideband. The other maximum point of interest, which is V_1=1.2V, is also referred as the MiTB, where the heterodyne process occurs due to the beating between the 20GHz sidebands as the CW signal is suppressed as explained above. The minimum mm-wave peak power are obtained at between -2V to -1V and 3.5V to 4.5V regions because of the bias at the quadrature point.

Lastly, the experiment is extended by transmitting the 1.25Gbps signal by directly modulating it into LD to test the credibility of the 40GHz carrier generated. The signal is then passed through the DSB-OCS system, which is connected to a 20km SMF and detected by a PD at the RAU. The 40GHz signal is amplified and then transmitted over the air by a 23dBi antenna before captured by a similar antenna, which is strategically placed in the line-of-sight position 4m from the first antenna. Subsequently, the captured 40GHz signal is down-converted to obtain back the 1.25Gbps and amplified for measurement purpose. Fig. 9 shows the BER versus received optical power for the recovered signal. It can be seen from the graph that 1.25Gbps signal has almost no penalty between the back to back and 20km fibre for a BER of 10^{-9}.

V. CONCLUSION

We have presented the characterisation results of DSB-OCS technique to generate 40GHz carrier for ROF system using DE-MZM. On top of that, MiTB has been used to suppress the optical carrier by 25dB. As a result, a 40GHz carrier can be generated with the amplitude up to -29dBm and SNR of 35dB by choosing specific optical power and RF driving power to the DE-MZM. The generated carrier is further tested for its credibility by transmitting 1.25Gbps signal through the DSB-OCS system. From the 5m wireless transmission assessment, an error free 40GHz ROF system has been achieved as almost no penalty is observed between the back to back and 20km fibre for a BER of 10^{-9}. The proposed system has great potential to be used in the future Gbps wireless access network.

ACKNOWLEDGMENT

The authors would like to thank TM R&D for providing the grant for this work under Project No:RDTC/110774. The authors also would like to acknowledge the Ministry of Higher Education Malaysia and the administration of Universiti Teknologi Malaysia (UTM) for the project financial support through Institutional Grant vote number 02H00.

REFERENCES

[1] Wake, D., Moodie, D. G. (1997), "Passive Picocell - Prospects For Increasing The Radio Range," in Proceeding of the International Topical Meeting on Microwave Photonics, Duisburg, 269 – 271.

[2] Seeds, A. J., Liu, C. P., Ismail, T., Fice, M. J., Pozzi, F., Steed, R. J., et al. (2010). Microwave photonics. Paper presented at the *Lasers and Electro-Optics/Quantum Electronics and Laser Science Conference: 2010 Laser Science to Photonic Applications, CLEO/QELS 2010,*

[3] Alwayn, V. (2004), Optical Network Design and Implementation, USA: Cisco Press.

[4] Stephens, T., Hinton, K., Anderson, T., & Clarke, B. (1995). Laser turn-on delay and chirp noise effects in Gb/s intensity-modulated direct-detection systems.*Journal of Lightwave Technology, 13*(4), 666-674.

[5] L. N. Langley, M. D. Elkin, C. Edge, M. J. Wale, X. Gliese, X. Huang, and A.J. Seeds, "Packaged Semiconductor Laser Optical Phase-Locked Loop (OPLL)for Photonic Generation, Processing and Transmission of Microwave Signals", IEEE Trans. On Microwave Theory and Techniques, Vol. 47, NO. 7, 1257 -1264, (1999).

[6] L. A. Johansson, and A. J. Seeds, "36 GHz 140-Mb/s Radio-Over-Fiber Transmission Using an Optical Injection Phase-Lock Loop Source", IEEE Photonics Tech. Letters Vol. 13, NO. 8, 893 - 895, (2001).

[7] Laurêncio, P., Vargues, H., Avó, R., & Medeiros, M. C. R. (2010). Generation and transmission of millimeter wave signals employing optical frequency quadrupling. Paper presented at the 2010 12th International Conference on Transparent Optical Networks, ICTON 2010.

[8] R. Mohamad, A.K. Zamzuri, S. Yaakob, S.M. Idrus, A.S. Supaat, "Internally Generated 21.6-GHz Millimeter Wave based on Brillouin Fiber Laser", 3rd International Conference on Electrical Engineering and Informatics (ICEEI 2011), Bandung, Indonesia, Paper ID: I3 – 4, July 17-19, 2011.

[9] Y. G. Shee, M. A. Mahdi, M. H. Al-Mansoori, S. Yaakob, R. Mohamed, A. K. Zamzuri, A. Man, A. Ismail, S. Hitam, "All-Optical Generation of 21 GHz Microwave by Incorporating a Double Brillouin Frequency Shifter", Optics Letters, Vol. 35, No. 9, pp. 1461 - 1463, 2010.

[10] Shee Yu Gang, M. A. Mahdi, M. H. Al-Mansoori, Nor Azura Ahmad Hambali, M. Z. Abdul Kadir, Romli Mohamad, Syamsuri Yaakob, "Threshold reduction of stimulated Brillouin scattering in Photonic crystal fiber", Laser Physic Journal, Vol. 19, No. 12, pp. 2194–2196, 2009.

[11] Hsueh, Y. -., Jia, Z., Chien, H. -., Yu, J., & Chang, G. -. (2009). A novel bidirectional 60-GHz radio-over-fiber scheme with multiband signal generation using a single intensity modulator. IEEE Photonics Technology Letters, 21(18), 1338-1340.

[12] Park, C. S., Yeo, Y. -., & Ong, L. C. (2010). Demonstration of the GbE service in the converged radio-over-fiber/optical networks. Journal of Lightwave Technology, 28(16), 2307-2314.

[13] Seo, J. -., Choi, C. -., Kang, Y. -., Chung, Y. -., Kim, J., & Choi, W. -. (2006). SOA-EAM frequency up/down-converters for 60-GHz bi-directional radio-on-fiber systems. IEEE Transactions on Microwave Theory and Techniques, 54(2), 959-966.

[14] Cao, Z., Yu, J., Zhou, H., Wang, W., Xia, M., Wang, J., et al. (2010). WDM-ROF-PON architecture for flexible wireless and wire-line layout. *Journal of Optical Communications and Networking, 2*(1-3), 117-121.